Anti-Phase Mode Isolation in Tuning-Fork MEMS using a Lever Coupling Design

Brenton R. Simon, Alexander A. Trusov, Andrei M. Shkel
MicroSystems Laboratory, Mechanical and Aerospace Engineering
University of California, Irvine, CA, USA
Email: brsimon@uci.edu, atrusov@uci.edu, ashkel@uci.edu

***Abstract*— A new coupling design is proposed and demonstrated for MEMS tuning-fork structures, which successfully isolates the anti-phase vibratory mode in both frequency and Q-factor. G-sensitivity is reduced by design through 1) creation of a high frequency separation between anti-phase and in-phase vibratory modes, 2) maximization of the in-phase resonance frequency, and 3) minimization of in-phase Q-factors. The proposed design accomplishes these goals by using a levering mechanism for coupling the proof masses, in contrast to a conventional approach via flexural spring. This structural design allows for large frequency separations between the anti-phase and in-phase vibratory modes, experimentally demonstrated up to 119% using a previously established quadruple mass gyroscope (QMG) [1]. Furthermore, due to the additional stress present within the lever coupling, in-phase Q-factors are reduced through tailored thermoelastic damping. The result is an anti-phase resonance separated in Q-factor and fQ product by over two orders of magnitude, compared to the in-phase mode. This is shown in comparison to an identical device with a spring coupling, demonstrated with a 25% frequency separation and one order of magnitude separation in both Q-factor and fQ product.**

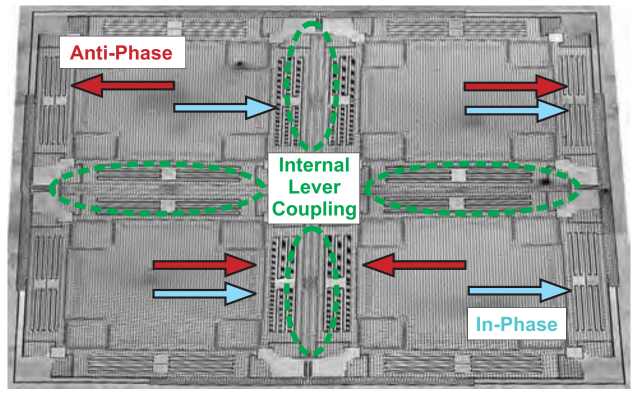

Fig. 1. Scanning electron microscope image of QMG with lever coupling.

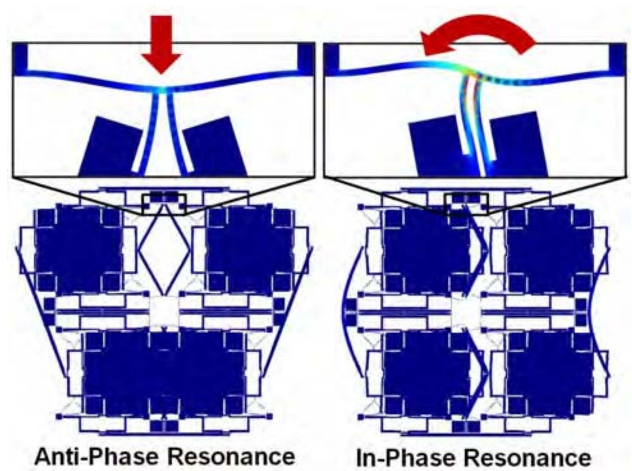

Fig. 2. Finite element modeling of quadruple mass gyroscope, showing the desired anti-phase vibratory mode (left) alongside the parasitic in-phase vibratory mode (right).

I. Introduction

For many dynamic MEMS, including gyroscopes and resonators, Q-factor is proportional to the amplitude of response and therefore sensitivity. Maximization of Q-factor is therefore desired for high-performance devices [1]. There are several challenges for the successful operation of high-Q sensors, one of which is sensitivity to external vibration and shock. Anti-phase operation of tuning-fork structures is a common method of reducing G-sensitivity of vibratory MEMS [2]; however, unavoidable structural asymmetry induced by fabrication imperfections hinders this approach by coupling the in-phase and anti-phase vibratory modes [3]. Mode ordering can be used to reduce this effect by increasing the frequency of the in-phase vibratory mode, separating it from the anti-phase resonance. While past designs have explored methods of stiffening the in-phase vibratory mode of tuning-fork structures [4][6], they required a large amount of surface area or wide etched cavities, potentially further increasing fabrication imperfections. For this reason, an alternative design is proposed that would not increase the critical etching dimension of the device. The new coupling design is able to achieving a high frequency separation while maintaining the critical low-frequency anti-phase resonance.

In addition to frequency isolation, isolation of the anti-phase Q-factor is beneficial to common-mode rejection as well. It has previously been established that structural asymmetries can result in energy transfer between vibratory modes. Proper mode ordering is therefore important for two reasons: 1) to reduce the initial transfer of energy into the in-phase resonance (high in-phase resonance), and 2) to reduce the transfer of energy from the in-phase to the anti-phase mode (high frequency separation). In order to reduce the energy that has already entered the in-phase modes, increased damping within these modes is ideal. For devices limited by thermoelastic damping,

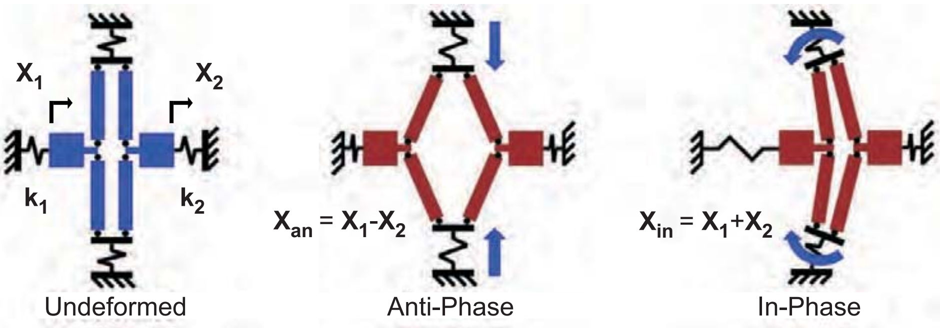

Fig. 3. Conceptual diagram of the proposed lever coupling mechanism (left). The flexures anchoring the lever coupling to the substrate are deflected through anti-phase motion (center), and torqued during in-phase motion (right). These flexures can be designed to produce different stiffness for each resonance.

increasing internal stress exacerbates this loss mechanism and can be accomplished with the leveraging structure.

II. Operation

A. Design Concept

Tuning-fork resonators consist of two or more masses, mechanically coupled to form a shared resonance. These masses can either move together, in-phase with one another, or in opposite directions, forming an anti-phase resonance, Figure 1. Typical tuning-fork resonators are coupled with a simple flexure spring, which is only deflected during anti-phase resonance. This forces the in-phase resonance to always be lower than the anti-phase mode due to the additional stiffness of the coupling.

Because both a high in-phase resonance and large frequency separation are ideal, one solution is to replace the spring coupling with a different structure capable of switching the order of the two vibratory modes. The chosen structure is comprised of four stiff levers attached to two clamped-clamped beams, Figure 4. During anti-phase resonance, Figure 3, the levers convert a large horizontal displacement into a small vertical displacement at the clamped-clamped beams. This deflects the beams into their first mode shape, Figure 2, imparting little additional stiffness to the resonance. During in-phase resonance, torque is applied to the clamped-clamped beams, Figure 3, forcing the clamped-clamped beams into their second mode shape, Figure 2, imparting both a greater stiffness, as well as greater stress throughout the attachment. Through proper design, this increase in stiffness within only the in-phase vibratory mode can be used to create a large frequency separation with respect to the anti-phase resonance.

B. Mode Ordering

The equations of motion of a dual-mass tuning-fork resonator can be transformed into in- and anti-phase resonances. Assuming zero damping and structural asymmetry within the flexures, it can be shown that the energy coupling between the modes is directly proportional to the stiffness mismatch [5]:

$$\begin{aligned} \ddot{x}_{an} + \omega_{an}^2 x_{an} &= \frac{\Delta k x_{in}}{2m} + \frac{F(t)}{2m} \\ \ddot{x}_{in} + \omega_{in}^2 x_{in} &= \frac{\Delta k x_{an}}{2m} + a(t) \end{aligned} \tag{1}$$

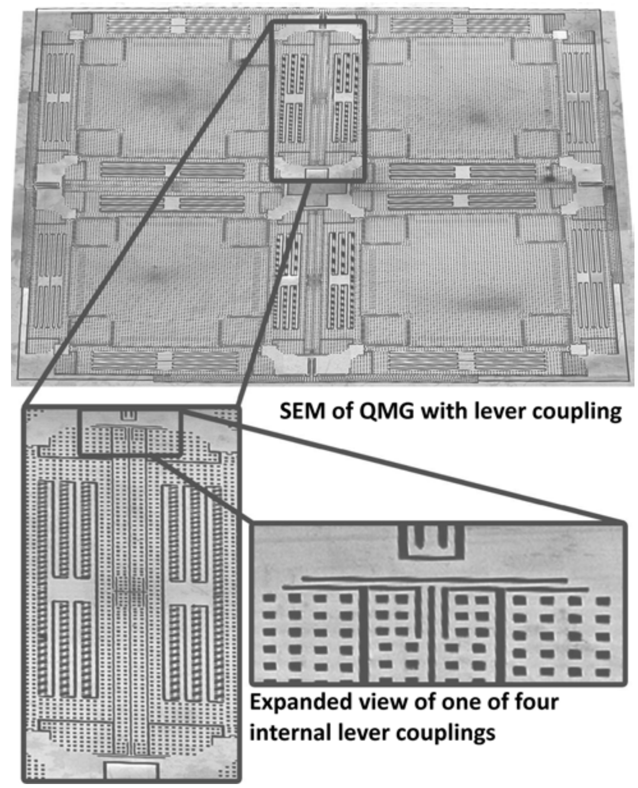

Fig. 4. Scanning electron microscope image of a quadruple mass gyroscope with internal lever coupling (top), zoomed image of lever coupling (bottom left), and zoomed image of clamped-clamped beam (bottom right).

where x_{an}, x_{in} and ω_{an}, ω_{in} are the modal displacement and natural frequencies of the anti-phase and in-phase modes, respectively, m is the mass of each proof mass, $\Delta k = k_1 - k_2$ is the stiffness mismatch, $F(t)$ is an anti-phase forcing function, and $a(t)$ is external acceleration. By increasing the in-phase resonance, ω_{in}, a lower in-phase amplitude is invoked for a fixed acceleration, which reduces the energy capable of transfer to the anti-phase resonance.

With further examination of the anti-phase equation of motion, along with neglecting the forcing function, the following equation can be derived relating the anti-phase response to energy coupling from the in-phase vibratory mode:

TABLE I

FINITE ELEMENT MODELING AND EXPERIMENTAL COMPARISON OF QUADRUPLE MASS GYROSCOPES WITH LEVER AND SPRING COUPLING DESIGNS

	Finite Element Modeling				Experimental					
	Lever Coupling		Spring Coupling		Lever Coupling			Spring Coupling		
Mode Shape	Freq. (Hz)	Q_{TED}	Freq. (Hz)	Q_{TED}	Freq. (Hz)	Q-factor	**Freq. Ratio**	Freq. (Hz)	Q-factor	**Freq. Ratio**
Anti-Phase (A)	2516	**1.49e6**	2614	**1.37e6**	1941	1.10e6	**1**	2156	8.96e5	**1**
In-Phase (B)	5008	2.87e4	3195	7.13e4	4255	3.90e3	**2.19**	2783	7.20e4	**1.29**
Hybrid (C)	3669	**2.82e4**	2516	**1.51e6**	2888	1.50e4	**1.49**	2054	3.22e5	**0.95**
Hybrid (D)	4252	5.78e4	3113	7.00e4	3649	4.90e3	**1.88**	2703	6.90e4	**1.25**

$$\frac{x_{an}}{x_{in}} = \frac{\Delta k}{2m(\omega_{an}^2 - \omega_{in}^2)} \quad (2)$$

In this equation, it is shown that energy transfer is minimized by maximizing the frequency separation.

C. Q-factor Isolation

While mode ordering can influence the transfer of energy, damping is needed to remove any energy after it has entered the in-phase resonance. Quickly eliminating this energy by minimizing the in-phase time constant, τ_{in}, reduces the effects on the anti-phase resonance:

$$\tau_{in} = \frac{Q_{in}}{\omega_{in}} \quad (3)$$

By reducing the in-phase Q-factor and increasing the in-phase frequency, the time required to dissipate any acquired energy is minimized.

III. FINITE ELEMENT ANALYSIS

A. Mode Ordering

The software COMSOL Multiphysics was used to numerically model quadruple mass gyroscopes with both lever and spring couplings. In each model, the entire device was simulated as single-crystal silicon with a Young's Modulus of 170 GPa and static mesh consisting of 80k triangular elements. The lowest four modes of each device consisted of similar mode shapes, though with varying frequencies: a complete anti-phase mode (A), a complete in-phase mode (B), and two hybrid modes sharing characteristics of each (C/D), Figure 5. The numerical results are presented in Table I. Notice that mode C is at a frequency lower than the anti-phase resonance for the spring coupling, and shifted to a higher frequency through the use of the new design. Stiffening this mode contributes to the increased stiffening of the complete in-phase mode (B), resulting in a higher frequency separation between the anti-phase and in-phase vibratory modes.

B. Q-factor Isolation

The finite element model was then used to assess the level of thermoelastic damping in each of the four resonances. Thermoelastic damping is a material-dependant loss mechanism, which can be calculated for a simple spring using the equation [7]:

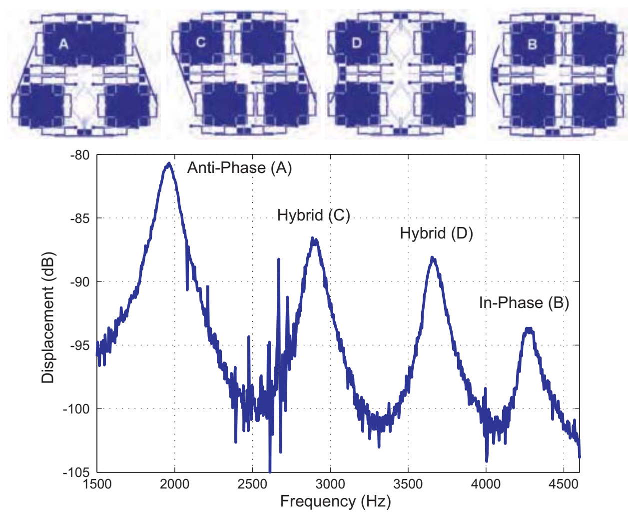

Fig. 5. Frequency response of quadruple mass gyroscope with lever coupling (bottom), along with finite element modeling of the lowest four vibratory modes: anti-phase (A), in-phase (B), and two hybrid (C/D).

$$Q_{TED} = \frac{E\alpha^2 T_0}{C_v} \frac{\omega_n \tau}{1 + \omega_n^2 \tau^2} \quad (4)$$

$$\tau = \frac{h^2 C_v}{\pi^2 k} \quad (5)$$

where α is the linear coefficient of thermal expansion, C_v is the specific heat per unit volume, k is the thermal conductivity, T_0 is the equilibrium temperature, E is the Young's Modulus, and h is the beam thickness. By discretizing this equation for use in COMSOL, the thermoplastic damping can be estimated for each of the four vibratory modes of interest, Table I. While each mode is not guaranteed to be limited by this loss mechanism, this calculation serves as an innate upper bound for the Q-factor. For the spring coupling, there are two vibratory modes with Q-factors in excess of 1 million: the anti-phase mode (A), and one of the hybrid modes (C). For the lever coupling, due to the larger frequency and increased stress, thermoelastic damping has been reduced in the hybrid mode (C) by nearly 2 orders of magnitude.

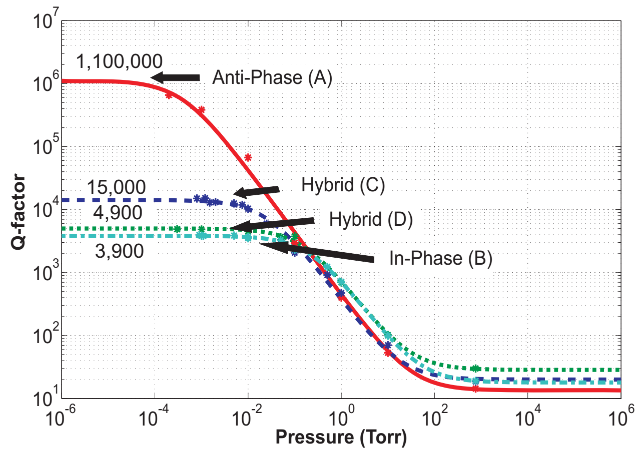

Fig. 6. Experimental Q-factor versus pressure of quadruple mass gyroscope with lever coupling.

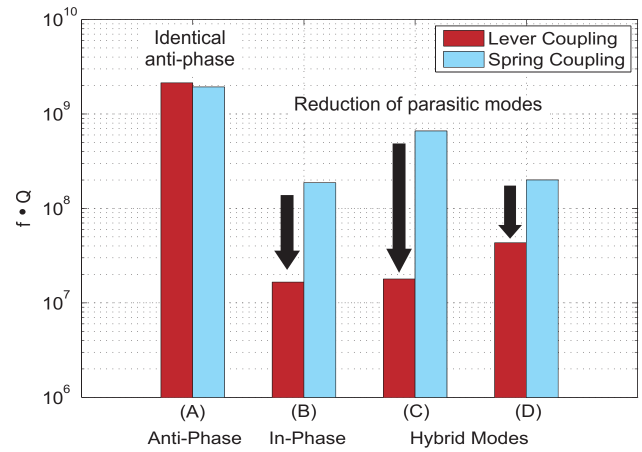

Fig. 7. Frequency / Q-factor product comparison of quadruple mass gyroscopes with lever and spring coupling. Four vibratory modes compared: anti-phase (A), in-phase (B), and two hybrid (C/D).

IV. Experimental Results

A. Mode Ordering

A silicon-on-insulator (SOI) fabrication process was used to create the proposed devices with a 100 μm device layer thickness, 5 μm minimum features, and a die size of 8x8 mm. Actuation and detection was accomplished through comb drive and parallel plate electrodes, respectively, attached to each proof mass. Using only the electrodes attached to a single proof mass, a frequency sweep was obtained to identify each of the four resonances, Figure 5. Each vibratory mode was confirmed by modifying the polarity of the additional electrodes to reflect each of the predicted mode shapes.

B. Q-factor Isolation

Quadruple mass gyroscopes are restricted by three primary loss mechanisms: viscous damping, anchor losses, and thermoelastic damping. In order to alleviate viscous damping, the spring-coupled device was vacuum sealed with getter material to achieve μTorr pressure levels. Data on the lever-coupled device was obtained in a vacuum chamber, capable of achieving 0.1 mTorr. By measuring the Q-factor of each vibratory mode at various pressure levels, the non-viscous damping Q-factors were identified, Figure 6.

Frequency and Q-factor naturally have an inverse relationship, therefore the above information was used to compare the fQ product of the two sensors, Figure 7. From this figure it can be seen that the anti-phase resonance has remained high for ideal sensor performance, while the in-phase modes have all been suppressed. In particular, the complete in-phase mode has been reduce by over an order of magnitude.

V. Conclusion

A lever coupling is described for implementation on tuning-fork structures, where anti-phase resonance is used to reduce anchor losses or vibrational sensitivity of the device. The improved coupling design has been shown to be capable of isolating the useful anti-phase resonance in frequency, as well as Q-factor for devices limited by thermoelastic damping. Unlike traditional spring couplings, the levering design can be used to stiffen the in-phase resonance of the structure, while leaving the anti-phase compliant. The high in-phase frequency reduces the transfer of energy into the device from external vibration, while the high frequency separation between the anti-phase and in-phase vibratory modes reduces the transfer of energy into the anti-phase resonance, affecting performance. Furthermore, by leveraging the displacement of the resonator to a high-stiffness clamped-clamped beam, a larger stress is imparted to the in-phase resonances, thus reducing the in-phase Q-factors due to thermoelastic damping. This serves as an upper bound to the Q-factors of these resonances and aids in quickly dissipating any in-phase motion, reducing the transfer of energy to the anti-phase mode. When compared to the conventional spring coupling, the proposed levering design maintains a compliant, high-Q, anti-phase resonance, while increasing the isolation of this mode from additional, parasitic resonances. The final result is a reduction in the fQ product by over one order of magnitude for the complete in-phase vibratory mode.

Acknowledgment

This work was supported by the ONR/NSWCDD grants N00014-09-1-0424 and N00014-11-1-0483. Devices were designed and characterized at the UC Irvine MicroSystems Laboratory. Fabrication was performed at the UC Irvine Integrated Nanosystems Research Facility and UC Los Angeles Nanolab.

References

[1] I.P. Prikhodko, S.A. Zotov, A.A. Trusov, A.M. Shkel, IEEE Transducers, 2011
[2] C.M. Jha, J. Salvia, A. Chandorkar, R. Melamud, E. Kuhl, T.W. Kenny, Applied Physics Letters, Appl. Phys. Lett. 93, 2008
[3] A.A. Trusov, S.A. Zotov, A.M. Shkel, IEEE Sensors, 2010
[4] K. Azgin, Y. Temiz, T. Akin, IEEE MEMS, 2007
[5] M. Weinberg, A. Kourepenis, JMEMS, 2006
[6] A. Walther, M. Savoye, G. Jourdan, P. Renaux, F. Souchon, P. Robert, C. Le Blanc, N. Delorme, O. Gigan, C. Lejuste, IEEE MEMS, 2012
[7] S. Prabhakar, S. Vengallatore, JMEMS, 2008
[8] T.P. Singh, K. Sugano, T. Tsuchiya, O. Tabata, IEEE Transducers, 2011